

Nonstatistical fragmentation of large molecules

M. H. Stockett,¹ H. Zettergren,¹ L. Adoui,^{2,3} J. D. Alexander,¹ U. Bērziņš,⁴ T. Chen,¹ M. Gatchell,¹ N. Haag,¹ B. A. Huber,² P. Hvelplund,⁵ A. Johansson,¹ H. A. B. Johansson,¹ K. Kulyk,¹ S. Rosén,¹ P. Rousseau,^{2,3} K. Støchkel,⁵ H. T. Schmidt,¹ and H. Cederquist¹

¹*Department of Physics, Stockholm University, Stockholm, SE-106 91, Sweden*

²*Centre de Recherche sur les Ions, les Matériaux et la Photonique (CIMAP), CEA-CNRS-ENSICAEN, F-14070 Caen Cedex 05, France*

³*Université de Caen Basse-Normandie, F-14032 Caen, France*

⁴*Institute of Atomic Physics and Spectroscopy, University of Latvia, Riga, LV-1586, Latvia*

⁵*Department of Physics and Astronomy, Aarhus University, DK-8000 Aarhus C, Denmark*

(Received 18 November 2013; published 6 March 2014)

We present experimental evidence for the dominance of prompt single-atom knockout in fragmenting collisions between large polycyclic aromatic hydrocarbon cations and He atoms at center-of-mass energies close to 100 eV. Such nonstatistical processes are shown to give highly reactive fragments. We argue that nonstatistical fragmentation is dominant for any sufficiently large molecular system under similar conditions.

DOI: [10.1103/PhysRevA.89.032701](https://doi.org/10.1103/PhysRevA.89.032701)

PACS number(s): 36.40.Qv, 34.50.Bw, 82.37.Np

Polycyclic aromatic hydrocarbons (PAHs) are of high current interest in several fields of research, e.g., combustion chemistry [1], environmental science [2], solar cell technology [3], molecular electronics [4], and astronomy [5]. PAHs and their clusters are believed to play key roles in soot formation processes [6] and are common air pollutants [7]. Observations of characteristic infrared emissions from different types of interstellar clouds and extragalactic sources strongly suggest that PAHs are present in many astronomical objects [8,9] where they may be subject to extreme fluxes of UV photons and energetic particles. Thus, it is important to understand the stability and destruction mechanisms of PAHs in different environments, as well as how their fragments may later react to form new molecules. Here we present a systematic investigation of how PAH cations of different sizes fragment in collisions with He atoms at center-of-mass energies close to 100 eV, a situation closely resembling the one where PAHs are exposed to supernova plasma shock waves in space [5,10]. Our results suggest that prompt, nonstatistical, single-atom knockout processes dominate the total fragmentation cross sections for PAHs containing more than 50 carbon atoms and for large molecules in general.

Internally heated molecules may relax by emitting photons, electrons, atoms, or molecules (fragmentation). When the internal excitation energy is statistically distributed across all internal degrees of freedom of the molecular system, the fragmentation channels with the lowest activation energies will dominate strongly. Such processes are commonly referred to as *statistical fragmentation* and are typically induced when molecules are first excited by absorption of one or several photons [11,12], or by the impact of energetic electrons [13], atoms [14], ions [15], or other particles. The molecules then decay after some time delay exceeding the typical vibrational time scale of picoseconds.

However, fragmentation may also occur before the excitation energy is distributed. When an atom collides with a molecule it may knock out one or several atoms in prompt, billiard-ball-like processes. For collisions involving *large* molecules, atom knockout processes have been directly observed only for collisions with C₆₀, but only in very

exceptional cases as small contributions to the fragmentation spectrum and only for *negatively charged* C₆₀ [16,17]. So far, knockout has not been identified for any neutral or positively charged large molecule isolated in vacuum. Yet, such *nonstatistical* fragmentation processes are expected to be important for a large range of collision systems [18]. As the lowest-energy dissociation channels are not necessarily favored, nonstatistical fragmentation yields different, more reactive fragments than statistical processes and may thus play an important role in the formation of larger molecules. This effect was recently observed in collisions between He²⁺ ions and clusters of C₆₀ molecules in which single carbon knockout from one C₆₀ molecule led to the formation of dumbbell-shaped C₁₁₉⁺ following C₅₉⁺ + C₆₀ bond-forming reactions [19].

It is in general very difficult to distinguish nonstatistical from statistical fragmentation processes for *large*, isolated molecules as they often have complex structures with many competing dissociation channels with similarly low activation energies. This situation is different for fullerenes and PAH molecules. These systems have lowest dissociation energies of about 10 eV (C₂ emission from fullerenes [20,21]) and 5–7 eV (H and C₂H₂ emission from the PAHs [22]). The dissociation energies for losses of single C atoms are substantially higher—typically 15 eV for fullerenes and 11–17 eV for PAHs depending on the position in the molecule but with similar values for different PAH sizes. Indeed, when PAHs are heated through interaction with photons [23], electrons [24], or high-energy ions [25], the H and C₂H₂-loss channels are dominant.

Thus, single C loss is typically insignificant in statistical fragmentation processes and should be a clear signature of nonstatistical knockout. In order to investigate how important this effect is for large molecules in general we have performed experiments with six planar PAH molecules ranging in size from that of anthracene C₁₄H₁₀ to coronene C₂₄H₁₂. For this purpose the PAHs have a huge advantage over the fullerenes as the probabilities of multiple knockout processes, or secondary knockouts by emitted carbon atoms, are much smaller for the PAHs for simple geometrical reasons. We are thus able

to unambiguously identify nonstatistical fragmentation by detecting the positively charged products in



reactions. The contribution from these knockout reactions is surprisingly large and becomes the dominant carbon-loss channel for large PAHs. From this result we infer that nonstatistical, single-atom knockout processes should become dominant for large molecules in general under similar conditions. We use density functional theory (DFT) calculations and Monte Carlo simulations of energy deposition processes to aid the interpretation of the results.

Continuous PAH⁺ cation beams were produced by electrospray ionization (ESI) following the sample preparation method of Marziarz *et al.* [26] and utilizing a custom radio-frequency ion funnel [27] to collect the ions. After mass selection by a quadrupole mass filter, the ions were accelerated and passed through a 4-cm-long collision cell containing the target gas. After the collision cell, a cylinder lens and two pairs of electrostatic deflector plates were used to analyze the fragment ions, which were recorded with a position-sensitive microchannel plate detector. Absolute total destruction cross sections were determined from the attenuations of the primary PAH⁺ beams as functions of the He pressure in the cell measured with a capacitance manometer. For the attenuation measurements, a set of narrow slits was placed in front of the detector such that the H-loss channels are included in the total PAH⁺ fragmentation cross sections.

In Fig. 1, we show fragment mass spectra for C₁₄H₁₀⁺ + He (present work) and He⁺ + C₁₄H₁₀ collisions (Holm *et al.* [25]) at center-of-mass energies of 110 eV and 11 keV, respectively. The initial location of the charge plays little or no role here as electron capture by He⁺ is the first step in the He⁺ + C₁₄H₁₀ collisions. Thus, in both cases, the positive charge will be located on the C₁₄H₁₀ (anthracene) molecule at small separations. Note the strong peak corresponding to the loss of a single carbon atom, marked -CH_x, in the present spectrum (black curve). The corresponding peak is very weak in the 11 keV spectrum [25] (gray curve) where the fragment distribution follows a bimodal intensity distribution that is

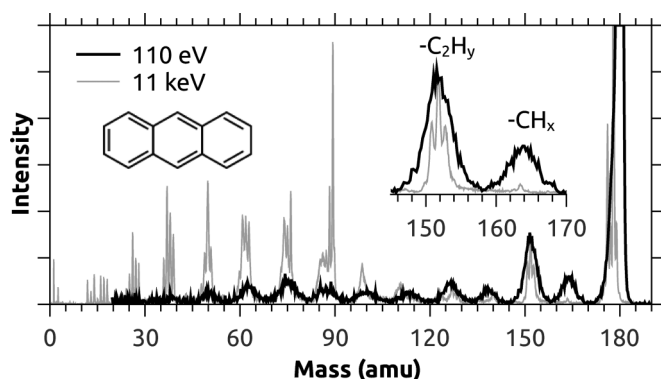


FIG. 1. Comparison of mass spectra due to C₁₄H₁₀⁺ + He (present work, black curve) and He⁺ + C₁₄H₁₀ ([25], gray curve) collisions at center-of-mass energies of 110 eV and 11 keV, respectively. Target densities were chosen to ensure single-collision conditions.

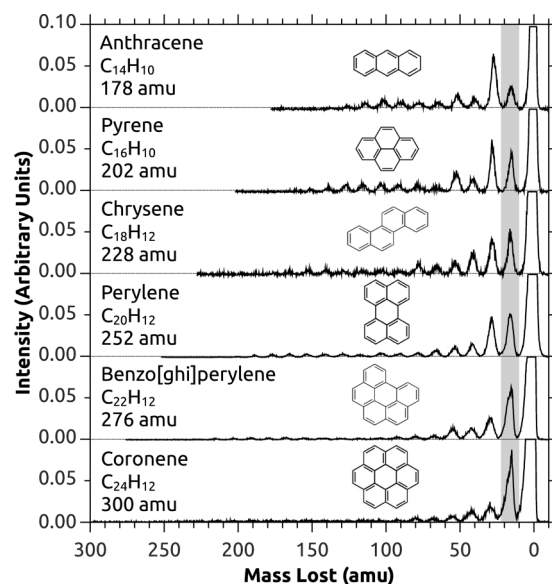


FIG. 2. Mass loss spectra for PAH⁺ + He collisions at 110 eV center-of-mass energy (see the text for details).

typical for collisions where electronic excitation energies are substantial. At 11 keV electronic excitations are about 40 eV [28] which results in statistical fragmentation of the PAHs [15]. In contrast, the prominent CH_x-loss peak in the present spectrum *cannot* be explained by statistical fragmentation (cf. [29,30]), as the energy barrier for C₂H₂ emission at about 4 eV [22] is much lower than the dissociation energies of 11–17 eV for the reactions in Eq. (1).

Following prompt knockout [Eq. (1)], the remaining energy in the molecule can induce further, statistical fragmentation. The excitation energy will depend only weakly on the PAH size as it is mainly deposited locally through nuclear and electronic stopping processes along the atom trajectories. Since larger PAHs have more vibrational degrees of freedom over which to distribute a given amount of energy, they are less likely to fragment further after knockout. This general trend is seen in the spectra in Fig. 2, which are normalized to the total integrated intensity of fragments having lost at least one carbon atom. The relative intensity of the CH_x-loss peak (highlighted in gray) increases with the mass of the PAH⁺ parent ion, and is clearly dominant for coronene. The C₂H_y-loss peak, on the other hand, decreases with increasing PAH size and is probably mostly due to statistical emission of C₂H₂ molecules. It is unlikely that the C₂H_y-loss peak results from decay of [PAH-CH_x]⁺ fragments, as PAHs with odd numbers of carbon atoms also typically dissociate via emission of C₂H₂ units [31].

In Fig. 3(a), we show examples of PAH⁺ attenuation measurements for three PAH⁺ cations in He. The attenuation of coronene cations (Cor⁺) in He, Ne, Ar, and Xe is shown in Fig. 3(b). In Fig. 3(c), we compare our measured absolute PAH⁺ destruction cross sections (including the H-loss channels) with calculated total and nonstatistical fragmentation cross sections based on a Monte Carlo model of electronic and nuclear stopping processes for random He trajectories through the PAHs. The nuclear energy transfers are calculated for He + C and He + H collisions in the PAHs using the screened

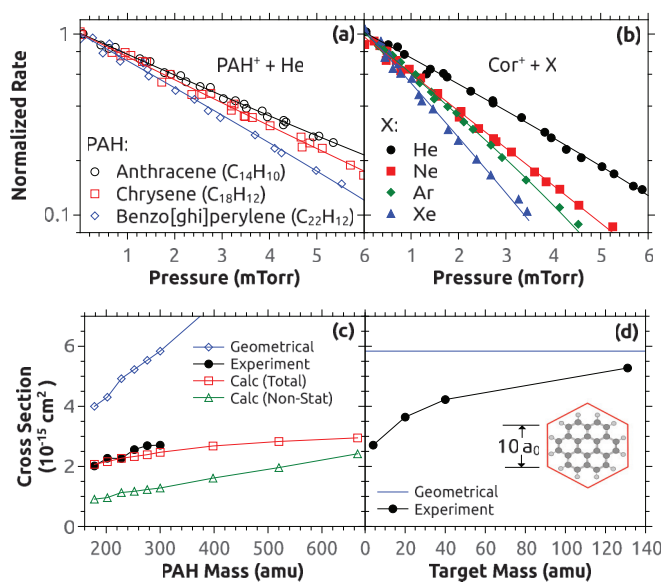


FIG. 3. (Color online) (a) Attenuation of PAH⁺ cation beams in He. (b) Attenuation of coronene cation beams in He, Ne, Ar, and Xe. The lines in (a) and (b) are single-exponential fits. (c) Experimental absolute PAH⁺ fragmentation cross sections for collisions with He at 110 eV center-of-mass energy, geometrical cross sections, and calculated absolute total and nonstatistical fragmentation cross sections (see text). (d) Experimental absolute Cor⁺ fragmentation cross sections for He, Ne, Ar, and Xe at a Cor⁺ laboratory energy of 8.35 keV. Statistical uncertainties are smaller than the experimental data points and lines between the points in (c) and (d) are to guide the eye.

Bohr potential [16] and the Ziegler-Biersack-Littmark (ZBL) potential [32], and the method described by Larsen *et al.* [16]. The electronic stopping contributions are calculated following Postma *et al.* [28] where we use the friction coefficients from Ref. [33] to obtain the electronic energy loss of He atoms traversing the PAH electron clouds [34]. We compare the resulting *total* energies with direct measurements of the energy required for statistical fragmentation for anthracene (C₁₄H₁₀) which was found to be 10 eV for a time window of tens of microseconds [35]. We then obtain the total fragmentation cross sections from the fraction of trajectories which give total stopping energies of at least $[(3N - 6)/36] \times 10$ eV for a PAH containing N atoms *or* nuclear stopping above the energy thresholds for knockout. The latter are taken to be 27 and 9 eV for single C- and single H knockout, respectively. These values are based on molecular dynamics (MD) simulations of He + C₁₄H₁₀ collisions by Postma *et al.* [36], which are consistent with MD simulations of ion impacts on graphene sheets [37] and the cross sections for electron-induced carbon knockouts from graphene [38]. The knockout cross section is related to the probability that the total stopping energy transferred to a given atom exceeds the threshold for removing that atom. The nonstatistical (knockout) cross sections obtained using the ZBL potential are shown in Fig. 3(c) for PAHs ranging in size up to that of circumcoronene (C₅₄H₁₈), a prototypical interstellar PAH [9]. The screened Bohr potential gives close to identical results (not shown). The experimental and the calculated cross sections lie substantially

below the geometrical cross section—i.e., an estimate of the total PAH⁺ fragmentation cross section assuming that all hits of the molecule lead to fragmentation. This shows that PAHs are partially transparent to He at the present collision energies.

Our calculations, which are in excellent agreement with our experimental data, indicate that $\geq 50\%$ of the total cross section is due to nonstatistical fragmentation for chrysene (C₁₈H₁₂) and all larger PAHs. The model predicts that nonstatistical fragmentation strongly dominates ($>80\%$) for circumcoronene (C₅₄H₁₈). When the total energy required for statistical fragmentation of a PAH containing N atoms is larger than the knockout threshold energies, which are independent of N , the knockout process will be the only relevant fragmentation pathway. For collisions with He at 110 eV, this will be the case for $N > 80$, which roughly corresponds to circumvalene (C₆₆H₂₀).

In Fig. 3(d), we show the absolute total destruction cross sections for coronene cations in collisions with He, Ne, Ar, or Xe target gases at a fixed PAH⁺ laboratory energy of 8.35 keV. As the target mass increases, the cross section approaches the naive estimate of the geometrical area of the molecule, taken to be a hexagon with a side length of $10a_0$ and considering the random orientation effect. For the heavier atoms, collisions in which sufficient energy is deposited to induce knockout can occur at larger distances from individual C or H atoms, and thus the “transparency” decreases with the mass of the target.

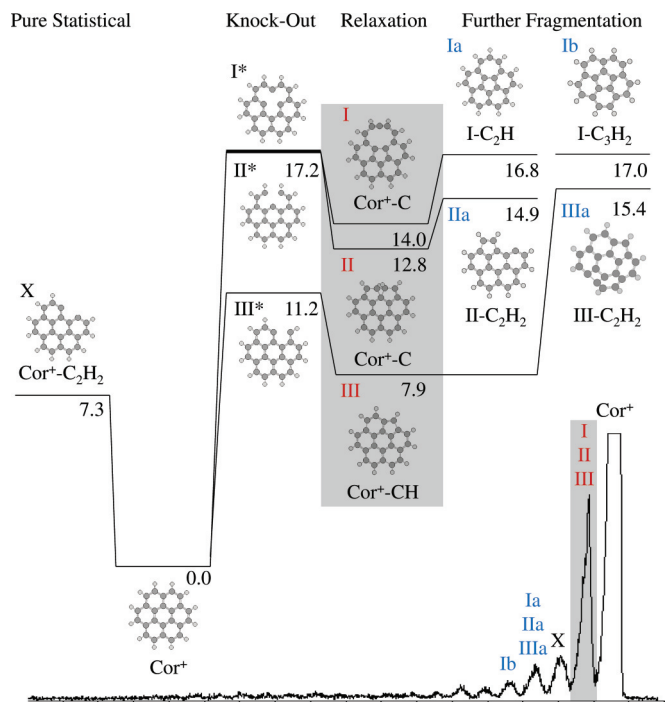


FIG. 4. (Color online) Likely structures of fragments produced by carbon knockout from coronene (C₂₄H₁₂, Cor⁺). The numbers indicate DFT energies (in eV) for the respective separated systems in relation to the ground state of Cor⁺. The labels I, II, III, etc. also indicate the fragment peaks to which they contribute. The gray area highlights structures which may contribute to the CH_x-loss peak. Structure X may result from C₂H₂ loss in a purely statistical process.

In Fig. 4, we show the mass spectrum for collisions between coronene and He as well as the results from DFT calculations using the B3LYP functional and the 6-311++G(2d,p) basis set as implemented in the GAUSSIAN09 package [39]. The structures correspond to intact and fragment ions which may contribute to the mass spectrum, where the energies are given relative to that of the intact coronene cation (Cor^+) in eV. While the potential energy surfaces of all possible fragments have not been fully explored, the structures presented should indeed be among the most likely products. Structures I*, II*, and III* are unrelaxed and used to estimate the energy difference for removing a carbon atom from three different positions in coronene—an inner C attached to three other carbon atoms, an outer C attached to three other carbon atoms, and an outer C attached to one hydrogen and two carbon atoms. These could relax to structures I, II, and III, respectively, all of which are thermodynamically stable and may contribute to the single carbon-loss peak highlighted in gray in Fig. 4. Additional energy remaining in systems I, II, and III may result in further, statistical fragmentation. Structure I, for example, may dissociate via emission of a C_2H or C_3H_2 unit with a dissociation energy less than the calculated relaxation energy, resulting in structures Ia and Ib, respectively. Likewise II may emit a C_2H_2 to give IIa. The dissociation energy for C_2H_2 loss from structure III is considerably higher. Structure X is one possible result of statistical C_2H_2 emission due to collisions where no knockout occurs, but sufficient energy is deposited through nuclear and electronic stopping for dissociation to be observed on the experimental time scale of tens of microseconds.

Note that structure I has a nine-membered ring and is expected to be much more reactive than PAHs containing only five- or six-membered rings. Recent theoretical studies of defects in graphene have shown that the binding energy for phenyl radicals (C_6H_5) to atoms near such defects increases by up to an order of magnitude compared with intact graphene [40]. Reactive fragments formed through knockout may be an important intermediate step in the bottom-up formation

of larger molecules such as the fullerenes [19,41] and nitrogen-substituted PAHs (PAHNs) [42]. The highly efficient carbon knockout process presented here could also play an important role in a top-down model of fullerene formation. It has been suggested that graphene or large PAHs (>60 C atoms) may be processed into three-dimensional structures like C_{60} in certain interstellar environments [43]. Structure Ib is corannulene, a three-dimensional bowl-shaped molecule which resembles a part of a fullerene cage. Structure IIIa is also bowl shaped. It is highly unlikely that such structures would be formed from coronene through purely statistical fragmentation resulting from, e.g., photoabsorption.

In this paper, we have shown an increasing prominence of the energetically highly disfavored CH_x -loss channel with increasing PAH mass in 110 eV $\text{PAH}^+ + \text{He}$ collisions. This is unambiguous evidence for the importance of nonstatistical fragmentation processes, and we estimate that it is the dominant decay pathway for interstellar PAHs containing more than 50 carbon atoms at typical supernova shock wave energies [9]. Nonstatistical fragmentation is expected to be important, and in some cases even dominant, when atoms or other heavy particles collide with large molecules in general at energies of a few tens to a few hundreds of eV. We have demonstrated that nonstatistical fragmentation leads to characteristic, unique, and often highly reactive fragments.

This work was supported by the Swedish Research Council (Contracts No. 621-2012-3662, No. 621-2012-3660, and No. 621-2011-4047). We acknowledge the COST Action CM1204 “XUV/X-ray light and fast ions for ultrafast chemistry (XLIC)” and computer time from CCCUAM and BSC Mare Nostrum. The work was partially supported by Projects No. FIS2010-15127, No. CTQ2010-17006, No. CSD2007-00010 (MICINN), No. S2009/MAT1726 (CAM), and the CNRS No. PICS-05356. U.B. was supported by the project FOTONIKA-LV, FP7-REGPOT Contract No. 285912. The authors acknowledge M. Larsson for his useful comments on this manuscript.

-
- [1] H. Richter and J. Howard, *Prog. Energy Combust. Sci.* **26**, 565 (2000).
- [2] K. Srogi, *Environ. Chem. Lett.* **5**, 169 (2007).
- [3] X. Wang, L. Zhi, N. Tsao, Ž. Tomović, J. Li, and K. Müllen, *Angew. Chem.* **120**, 3032 (2008).
- [4] S. Kubatkin, A. Danilov, M. Hjort, J. Cornil, J.-L. Brédas, N. Stühr-Hansen, P. Hedegård, and T. Bjørnholm, *Nature (London)* **425**, 698 (2003).
- [5] A. G. G. M. Tielens, *Rev. Mod. Phys.* **85**, 1021 (2013).
- [6] M. Frenklach, *Phys. Chem. Chem. Phys.* **4**, 2028 (2002).
- [7] B. J. Finlayson-Pitts and J. N. Pitts, *Science* **276**, 1045 (1997).
- [8] H.-S. Kim, D. R. Wagner, and R. J. Saykally, *Phys. Rev. Lett.* **86**, 5691 (2001).
- [9] A. G. G. M. Tielens, *Annu. Rev. Astron. Astrophys.* **46**, 289 (2008).
- [10] E. R. Micelotta, A. P. Jones, and A. G. G. M. Tielens, *Astron. Astrophys.* **510**, A36 (2010).
- [11] S. Martin, J. Bernard, R. Brédy, B. Concina, C. Joblin, M. Ji, C. Ortega, and L. Chen, *Phys. Rev. Lett.* **110**, 063003 (2013).
- [12] K. Hansen and O. Echt, *Phys. Rev. Lett.* **78**, 2337 (1997).
- [13] D. Hathiramani, K. Aichele, W. Arnold, K. Huber, E. Salzborn, and P. Scheier, *Phys. Rev. Lett.* **85**, 3604 (2000).
- [14] K. A. Caldwell, D. E. Giblin, and M. L. Gross, *J. Am. Chem. Soc.* **114**, 3743 (1992).
- [15] A. Ławicki, A. I. S. Holm, P. Rousseau, M. Capron, R. Maisonnay, S. Maclot, F. Seitz, H. A. B. Johansson, S. Rosén, H. T. Schmidt, H. Zettergren, B. Manil, L. Adoui, H. Cederquist, and B. A. Huber, *Phys. Rev. A* **83**, 022704 (2011).
- [16] M. C. Larsen, P. Hvelplund, M. O. Larsson, and H. Shen, *Eur. Phys. J. D* **5**, 283 (1999).
- [17] S. Tomita, P. Hvelplund, S. B. Nielsen, and T. Muramoto, *Phys. Rev. A* **65**, 043201 (2002).
- [18] T. Kunert and R. Schmidt, *Phys. Rev. Lett.* **86**, 5258 (2001).

- [19] H. Zettergren *et al.*, *Phys. Rev. Lett.* **110**, 185501 (2013).
- [20] S. Tomita, J. U. Andersen, C. Gottrup, P. Hvelplund, and U. V. Pedersen, *Phys. Rev. Lett.* **87**, 073401 (2001).
- [21] L. Chen, S. Martin, J. Bernard, and R. Brédy, *Phys. Rev. Lett.* **98**, 193401 (2007).
- [22] A. I. S. Holm, H. A. B. Johansson, H. Cederquist, and H. Zettergren, *J. Chem. Phys.* **134**, 044301 (2011).
- [23] S. P. Ekern, A. G. Marshall, J. Szczepanski, and M. Vala, *J. Phys. Chem. A* **102**, 3498 (1998).
- [24] M. E. Wacks and V. H. Dibeler, *J. Chem. Phys.* **31**, 1557 (1959).
- [25] A. I. S. Holm, H. Zettergren, H. A. B. Johansson, F. Seitz, S. Rosén, H. T. Schmidt, A. Ławicki, J. Rangama, P. Rousseau, M. Capron, R. Maissonny, L. Adoui, A. Méry, B. Manil, B. A. Huber, and H. Cederquist, *Phys. Rev. Lett.* **105**, 213401 (2010).
- [26] E. P. Maziarz III, G. A. Baker, and T. D. Wood, *Can. J. Chem.* **83**, 1871 (2005).
- [27] R. R. Julian, S. R. Mabbett, and M. F. Jarrold, *J. Am. Soc. Mass Spectrom.* **16**, 1708 (2005).
- [28] J. Postma, S. Bari, R. Hoekstra, A. G. G. M. Tielens, and T. Schlathölter, *Astrophys. J.* **708**, 435 (2010).
- [29] R. Arakawa, M. Kobayashi, and T. Nishimura, *J. Mass Spectrom.* **35**, 178 (2000).
- [30] S. J. Pachuta, H. I. Kenttamaa, T. M. Sack, R. L. Cerny, K. B. Tomer, M. L. Gross, R. R. Pachuta, and R. G. Cooks, *J. Am. Chem. Soc.* **110**, 657 (1988).
- [31] F. Seitz, A. Holm, H. Zettergren, H. Johansson, S. Rosén, H. Schmidt, A. Ławicki, J. Rangama, P. Rousseau, M. Capron, R. Maissonny, A. Domaracka, L. Adoui, A. Méry, B. Manil, B. Huber, and H. Cederquist, *J. Chem. Phys.* **135**, 064302 (2011).
- [32] J. F. Ziegler, J. P. Biersack, and U. Littmark, *The Stopping and Range of Ions in Matter* (Pergamon, Oxford, 1985), Vol. 1.
- [33] M. J. Puska and R. M. Nieminen, *Phys. Rev. B* **27**, 6121 (1983).
- [34] F. Seitz *et al.*, *J. Chem. Phys.* **139**, 034309 (2013).
- [35] S. Martin, L. Chen, R. Brédy, G. Montagne, C. Ortega, T. Schlathölter, G. Reitsma, and J. Bernard, *Phys. Rev. A* **85**, 052715 (2012).
- [36] J. Postma, R. Hoekstra, A. G. G. M. Tielens, and T. Schlathölter, *Astrophys. J.* **783**, 61 (2014).
- [37] O. Lehtinen, J. Kotakoski, A. V. Krasheninnikov, A. Tolvanen, K. Nordlund, and J. Keinonen, *Phys. Rev. B* **81**, 153401 (2010).
- [38] J. C. Meyer, F. Eder, S. Kurasch, V. Skakalova, J. Kotakoski, H. J. Park, S. Roth, A. Chuvilin, S. Eyhusen, G. Benner, A. V. Krasheninnikov, and U. Kaiser, *Phys. Rev. Lett.* **108**, 196102 (2012).
- [39] M. J. Frisch *et al.*, Gaussian 09 Revision A.1, Gaussian Inc. Wallingford CT, 2009.
- [40] P. A. Denis and F. Iribarne, *J. Phys. Chem. C* **117**, 19048 (2013).
- [41] J. Maul, T. Berg, E. Marosits, G. Schönhense, and G. Huber, *Phys. Rev. B* **74**, 161406 (2006).
- [42] T. Chen (unpublished).
- [43] O. Berné and A. G. G. M. Tielens, *Proc. Natl. Acad. Sci. USA* **109**, 401 (2012).